Influence of Liquid Viscosity and Solid Load in a Three-Phase Bubble Column using Stereoscopic Particle Image Velocimetry (Stereo-PIV)

Diana. I. Sanchez-Forero, Karina K. Costa, Rodrigo. L. Amaral, Osvaldir P. Taranto, Milton Mori*

School of Chemical Engineering, University of Campinas, UNICAMP, Av .Albert Einstein, 500, CEP: 13083-970, Campinas, SP, Brazil
mori@feq.unicamp.br

The bubble motion in non-Newtonian fluids is extensively used in many industrial processes. The influence of the liquid viscosity in the hydrodynamic behaviour of bubble columns is related to the bubble formation processes and the tendency to coalescence. In addition, the solids distribution through the column affects the system characteristics. The objective of this study is to evaluate the effect of the liquid properties and the influence of the solid phase on the bubble column hydrodynamic characteristics for a three-phase system. The experimental studies were carried out in a cylindrical bubble column laboratory scale with 145 mm internal diameter and a height of 1m. The three-phase system is consisted as follows: air as gas phase, solution of Carboxymethyl Cellulose (CMC) with liquid phase weight percentage of 0.25 wt%, and FCC particles with particle diameter of 100-125 μm. The air was injected at the bottom of the column using a gas sparger with 21 holes of 1mm diameter each, disposed in the central region of the column. For all the experiments were used an initial liquid height of 0.8 m and gas flow rate of 1.5 L/min. The effect of the viscosity and solid load under mean liquid velocity was measured using a non-intrusive technique Stereo Particle Image Velocimetry (Stereo-PIV) with Rhodamine B as a tracer particle. The results for a non-Newtonian solution (CMC) and solid load are presented and discussed.

1. Introduction

Multiphase systems (gas-liquid-solid) are widely used in several technologies for their high industry applicability in chemical, petrochemical and biochemical processing (Yang et al. 2007). Its importance is related to understanding the hydrodynamics and the effects for scale up three-phase systems. For example, the liquid viscosity effect in the system is related to the bubble formation processes and the tendency to coalescence (Kantarci et al. 2005). Moreover, the presence of the solid phase influences the gas-liquid system in relation to the bubble formation, rise bubble velocity, the mass transfer phenomena, porosity, flow regimens and liquid velocity profiles (Ruzicka, 2005).To investigate the bubble column hydrodynamic behavior it is used sophisticated image analysis techniques that allows determining velocity fields and analyzing flow structures (Bröder and Sommerfeld, 2007). Stereoscopic Particle Image Velocimetry (Stereo-PIV) is a non-intrusive technique that used two cameras to reconstruct the third component of flow velocity proving a 2D-3C velocity field (Prasad, 2000). This technique uses florescent tracer particles and a high-pass filter on each camera to measure only the velocity field of liquid phase.

1.1 Case of Study

This work consists in the study of three-phase flow in a cylindrical bubble column for 1. 5 L/min gas flow rate using the Fluorescent Stereo-PIV. The data obtained in the three phase system (CMC-FCC particles -air) it was compared with air- water-FCC particles system. The liquid viscosity (CMC solution) and load solid (FCC particles) effect on the bubble column hydrodynamic characteristics is analyzed.

2. Experimental Unit

2.1 Experimental facility
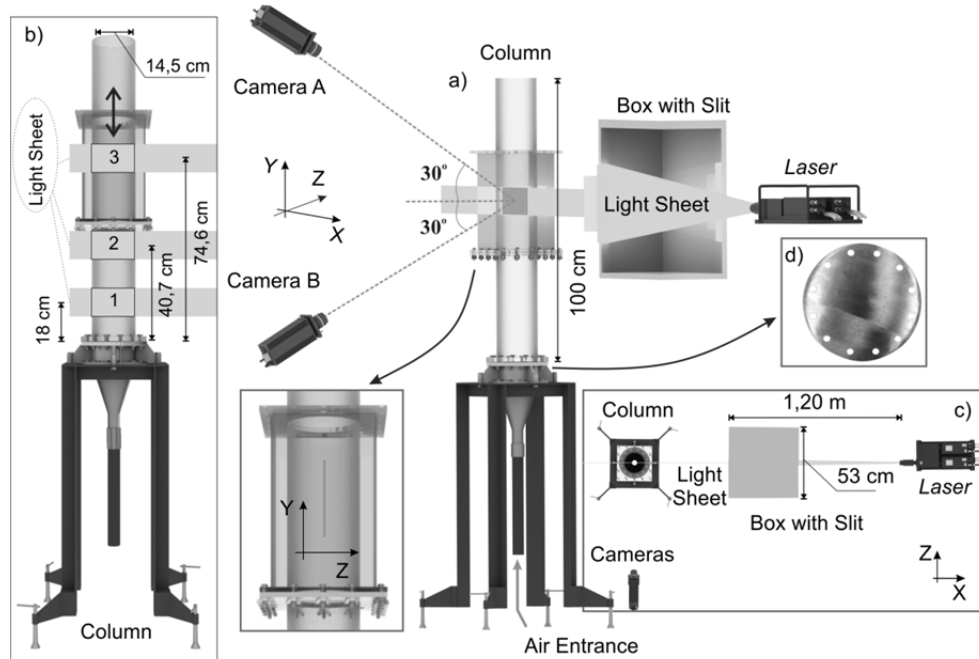The experimental facility used is showed in Figure 1.

Figure 1: (a) Column, laser system, box with slit and Stereo-PIV System. (b) Fields of view (c) Details of box with slit. (d) Gas distributor

The cylindrical bubble column is a transparent acrylic column of 14.5 cm of diameter and 1 m of high. The gas feed is performed by 21 holes of 1 mm of inner diameter disposed in the central region of the column bottom (Figure 1 (d)). The air (gas) rises, forming bubbles which are distributed throughout the liquid domain. The testes are performed with two different fluids as liquid phase: water at 25°C and solution of *Carboxymethyl Cellulose* (CMC) with liquid phase weight percentage of 0.25 wt%. The rheological properties of the CMC were measuring using a Haake Rheostress (RS1) rheometer with a shear stress range (τ) of 0.001 Pa-300 Pa. The experimental dates were adjusted by the Carreu-Yasuda model (Eq1):

$$\frac{\mu\text{-}\mu_0}{\mu_0\text{-}\mu_\infty} = \frac{1}{\left(1+(\lambda\dot\gamma)^a\right)^{1-n/a}} \tag{1}$$

The values for each parameter of the equation for a CMC solution (0.25 %wt) are: μ_0 =0.2107 (Pas), μ_∞ = 0.001 (Pas), λ= 0.9612 (s), a=0.3292 and n =0.6534.The measurements are performed around three sections of the column at 18, 40.7 and 74.6 cm of the injection section, respectively (Figure 1 (b)). The initial liquid high is 80 cm. As solid phase are used FCC particles with particle diameter of 100-125 µm. The FCC particles are added when the system is stable with a solid load of 10 g. The data is obtained for a gas flow rate of 1.5 L/min. Other experiments are performed by varying the solid load to 15 g and measured at 16.5 cm of the injection section using an air-CMC-FCC particles system.

2.2 Stereo PIV
In order to collected 4000 double images to analyzed the liquid phase hydrodynamic performance, it is used a Stereo-PIV system with two CCD (Charge Couple Device) cameras and Nd:YAG laser system (200mJ/pulse and λ =532 nm). The images are obtained by seeding the liquid with fluorescent particles of Rhodamine B (dp = 20 - 50 µm e λ = 620 nm). The time between the pulsing of the two laser cavities (pulse separation) is adjusted according to the measurement velocity. The images were transferred digitally from the CCD cameras to the controlling (PTU-9) by the software Davis 7.2 and an image processing PC. It is used a Stereo- PIV angular configuration (angular displacement 30°) that allows obtaining the angular displacement and focus all the measurement volume (Figure 1(a)). Each camera has an objective lens with a focal length of 60 mm model Nikon Micro-Nikor (f / 2.8D) and a high-pass filter that only allows the passage of light with a wavelength close to that of Rhodamine. It is used a box with a slit to obtained a defined light thickness (1mm)

and intensity profile top-hat (Figure 1 (c)). In addition, it is used an acrylic box filled with water in the investigation area that reduce errors caused by the column curvature distortion. After recorder, the images are processed and then it is applied the cross-correlation procedure to determine the velocity distribution of the fluid. Table 1 show the main parameters used in the Stero-PIV system.

Table 1: Principal Parameters of Stereo-PIV setup

Parameter	Value
Time inter-frame (dt)	5000 μs
Maximum particle image displacement	15-20 pixels
Acquisition frequency	4.92 Hz
Pixel size	6.45 μm
Laser power	25-40%
Particle image diameter	2-3 pixels
Image resolution	10 pixels/mm
Field of view	14.5 x 10 cm
Calibration error	≈0.8 pixels

3. Results and discussion

The Figure 2, 3, and 4 shows the vector fields for the axial liquid velocity (Vy) for: a) air - water system, b) air – water – FCC particles (10 g) system, and c) air –water- FCC particles (15 g) system, obtained for three investigation regions of the bubble column.
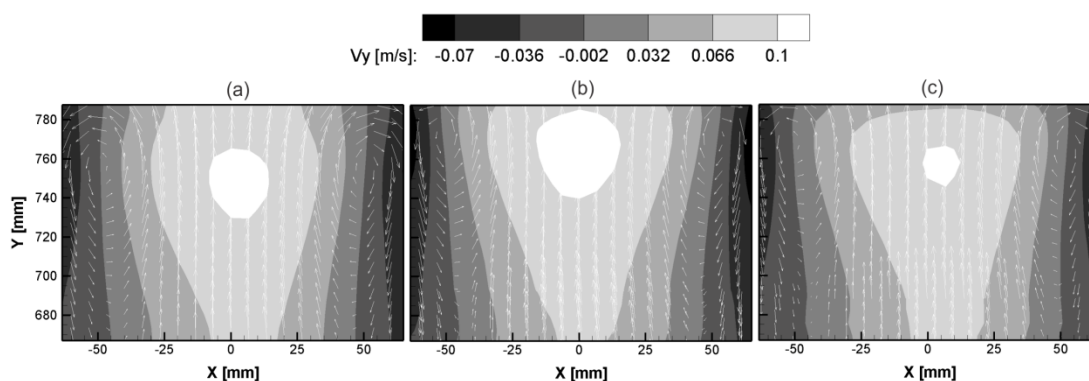

Figure 2: Vector field for liquid velocity Vy for: (a) air - water system, (b) air – water – FCC particles (10 g) system and (c) air –water- FCC particles (15 g) system at 732 mm of the injection section

In the Figure 2, it can be seen that the three systems demonstrate a developed flow. The recirculation areas are defined (vortex center at X= 25 [mm] and Y= 760 [mm] for the two-phase system). Although, this recirculation region becomes smaller with the addition of solid into the system (vortex beginning at region X= 27 [mm] for the three-phase system). The amount of solid in the walls region offers resistance to liquid circulation. The region of maximum liquid velocity decreases when more solid is added to the system (Figure 2 (c)). It can be explained because the solid is dispersed across the column and generates a resistance to the bubbles upward flow at the center of the column.

Figure 3 shows that the flow is developing, the liquid axial velocity decrease from the center towards the wall. The difference between the sizes of the regions can be explained for the solid concentration near the walls that is bigger than at the center of the column. This allows grater movement of bubbles through this area (less resistance caused by solid) and therefore higher liquid velocities.
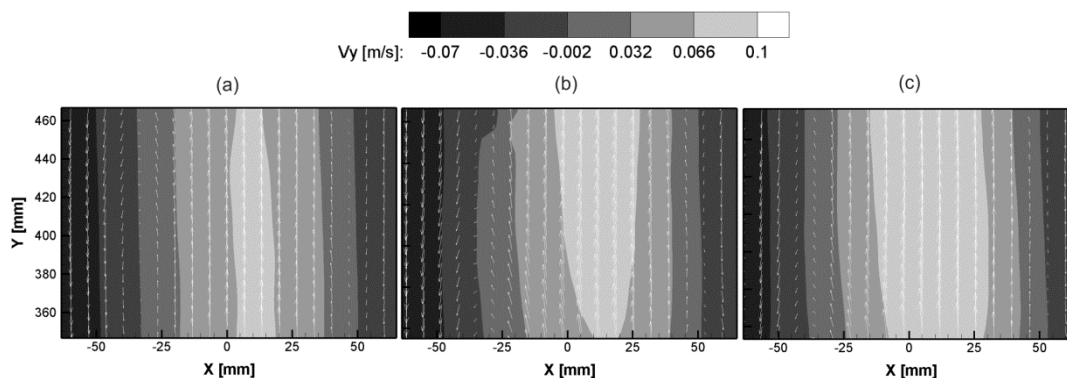
Figure 3: Vector field for liquid velocity Vy for: (a) air - water system, (b) air – water – FCC particles (10 g) system and (c) air –water- FCC particles (15 g) system at 392 mm of the injection section
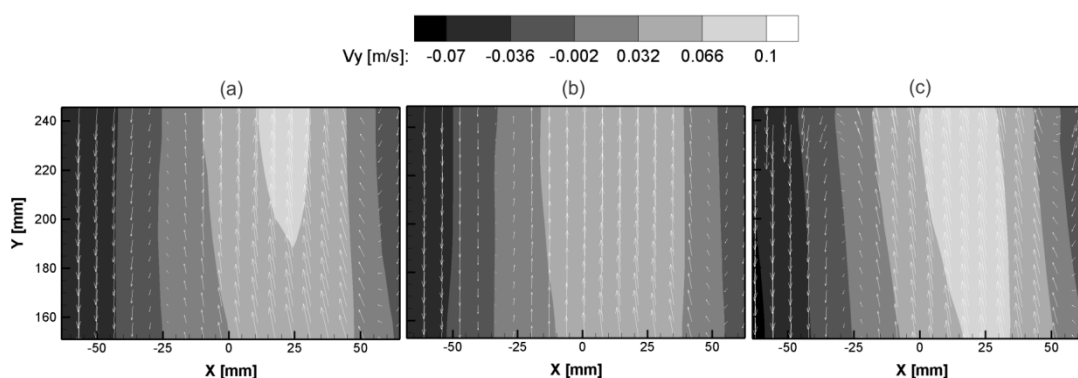

Figure 4: Vector field for liquid velocity Vy for: (a) air - water system, (b) air – water – FCC particles (10 g) system and (c) air –water- FCC particles (15 g) system at 165 mm of the injection section

The vector fields in the Figure 4 show a displacement of the liquid velocity vectors to the right side of the column due the aeration characteristics and low superficial gas velocity. The addition of the solid changes the structure of the flow. Note that by increasing the amount of solid until 15 g (Figure 4 (C)) the region of maximum liquid velocity appears. The solid is concentrated on the walls and allows the passage of liquid through the center of the column. However, when increasing in 10 g (Figure 4 (b)) the vectors seem linear. It can be concluded that for low superficial gas velocity, small solid load stabilize the system but this increase of solid has the opposite effect.

The Figure 5 shows the axial liquid mean velocity profile Vy for: (a) air - water system, (b) air – water – FCC particles (10 g) system and (c) air –water- FCC particles (15 g) system at three different heights (200, 400, and 700 mm). It can be observed that the axial mean liquid velocity profile changes with the column height. The profile is centralized at the top for the column, while near the bottom it is dislocated to the right (Figure 5). Besides, it can be seen that, in general, the liquid velocity increases with the height of the column because at the top exists less liquid above that allows the bubbles rises easily and then the liquid velocity is higher. Otherwise, the Figure 5 shows that the effect of the solid is more significant at the bottom of the column. Thus, at low solid load the particles-bubbles collisions lead to bubble velocity decrease in consequence less liquid velocity. When the profile is developed (Y=750 mm) it can be seen that the solid has no significant effect, and it can be explained for the small concentration of the solid added into the system.

The figure 6 shows the liquid flow vectors fields for: (a) air – CMC solution (25 %wt), (b) air CMC solution (25 %wt)– FCC particles (15 g) at 165 mm of the injection section, (c) air – CMC solution (25 %wt), (d) air CMC solution (25 %wt)– FCC particles (15 g) at 392 mm of the injection section, and (e) air – CMC solution (25 %wt), (f) air – CMC solution (25 %wt)- FCC particles (25 g) at 732 mm of the injection section. To analyzed the effect of the liquid viscosity (two- phase system), and the effect of the solid in a viscous solution (three-phase system) are compared the column behaviour at three different column height. It can be seen that the liquid viscosity has a significant effect in the structure of the flow (Figure 6 (a)) when it is compared with a water as liquid phase (Figure 3 (a)). The liquid velocity showed a strong displacement of the velocity vectors to the right side of the column with a biggest recirculation area (negatives velocities) from the center to left

column side. These phenomena can be explained because the bubbles have a preferential path due the low superficial gas velocity. When the height of measurement increase the flow is developed and the region of highs velocities increase too. The resistance of the liquid column is lower and the bubbles can rise with facility (Figures 6 (c) and 6(e)). The Figures 6 (b) and 6(d) showed the influence of the addition of the solid. Note that the solid presence to the system has a positive influence in the flow structure; the vectors tend toward to center. In the Figure 6 (f) it can be seen that the presence of the solid has influence on the system. The vectors are displacement to the left side, and the region with high velocity appears due the fact that the solid near the walls offers resistance to the bubble with upward movement in this region, which facilitates the passage of liquid through the center of the column. It can be seen recirculation areas in X = 25 mm.
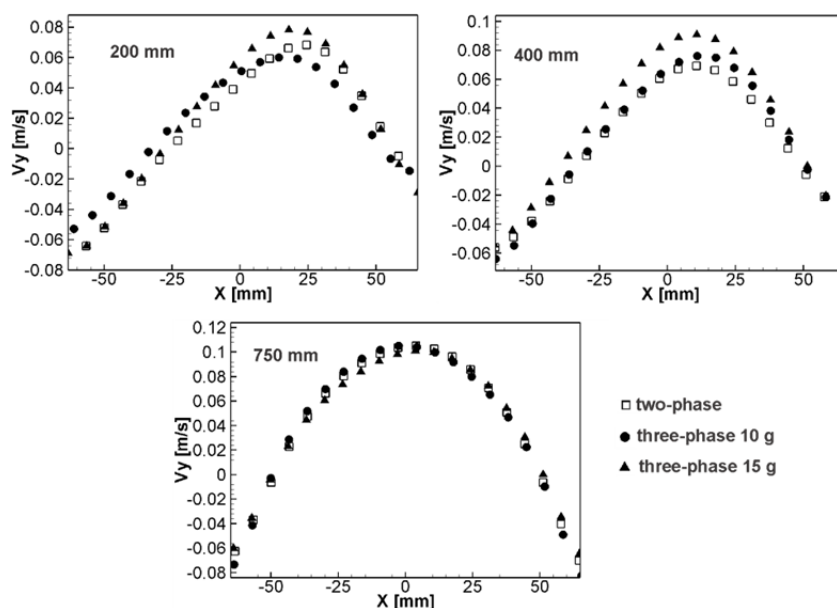

Figure 5: Axial liquid mean velocity profile Vy for: (a) air - water system, (b) air – water – FCC particles (10 g) system and (c) air –water- FCC particles (15 g) system at three different heights
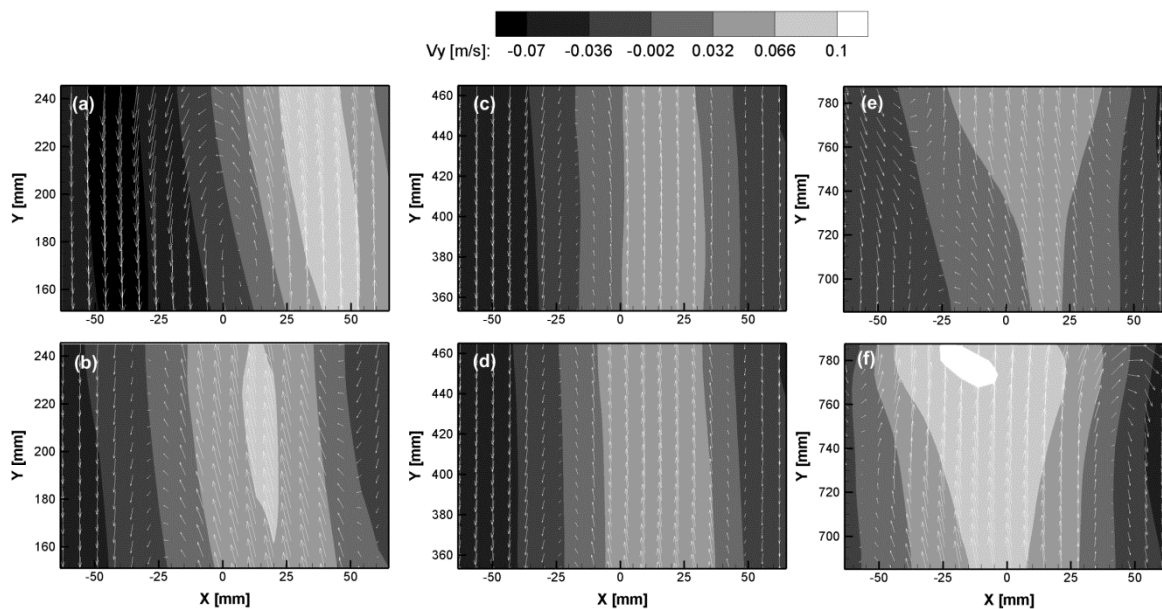

Figure 6: Vector field for liquid velocity Vy for different systems at three column heights from injection section

The Figure 7 show the axial liquid mean velocity profile Vy for: (a) air - water system, (b) air – CMC (0.25 % wt) and (c) air – CMC (0.25 % wt) - FCC particles (15 g) system at three different heights (200, 400, and 750 mm).
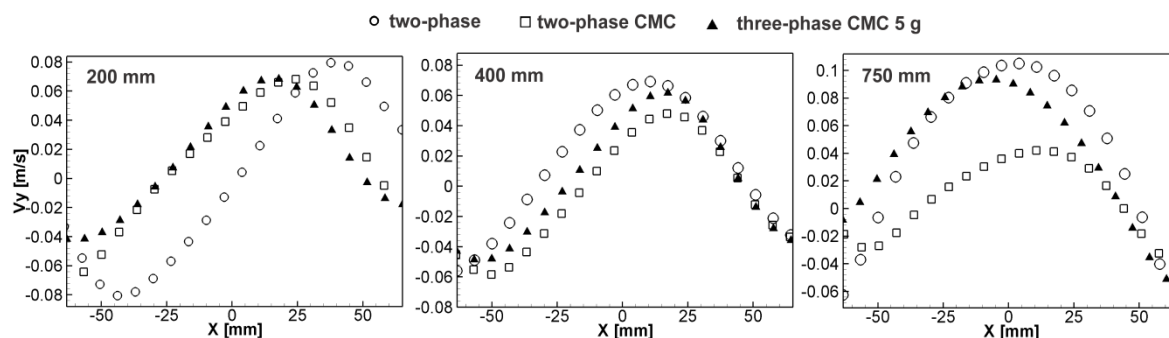

Figure 7: Axial liquid mean velocity profile Vy for: (a) air - water system, (b) air – CMC (25 % wt) c) air – CMC (25 % wt) - FCC particles (15 g) system at different heights

In Figure 7 it can be seen that for water as a liquid in the region near the bottom (Y = 200 mm), the bubbles kinetic energy is maximum and then the bubble velocity is higher. The liquid viscosity (CMC solution) and the addition of solid increase the viscous dissipation. The hydrodynamics forces and the collision bubble-particles reduce the bubbles velocity; promote the coalescence, and as a consequence the liquid velocity decrease. When the flow is developing, the influence of the viscosity is higher than that at the bottom (Y = 400 mm and Y = 750 mm) because the liquid velocity decrease as the liquid viscosity increase. When the solid is added to viscous solution, the liquid velocity is increased compared with the two-phase system (ar-CMC), reaching liquid velocities of 0.08 m/s. In all cases the liquid velocity profiles present the typical behavior for bubble columns, upward flow in the core region and a down-flow near the wall (Sanchez-Forero et al. 2013).

4. Conclusions

The experiments performed with Fluorescent Stereo- PIV provided data for fluid dynamics characterization. The experimental results show typical axial velocity profiles of the liquid, upward flow in the core region and a down-flow near the wall.
It was observed that the solid effect is significant in the column bottom where the flow is not developed; while at the top of the column it is not for the small concentration of the solid added into the system. Moreover, the liquid viscosity effect (two-phase flow) is higher. It can be observed that the liquid velocity decrease as the liquid viscosity increase, because the bubbles have an extra resistance that allow the movement upward. Besides, the viscosity promotes the bubble coalescence that affects the liquid velocity. However, the studied effects are not significant by the fact that the superficial gas velocity and solid load be low.

References
Bröder D., Sommerfeld M., 2007, Planar shadow image velocimetry for the analisys of the hidrodynamics in bubble flows, Meas. Sci. Technol., 18, 2513-2528.
Kantarci N., Borak F., Ulgen K.O., Gierer M., Ertl G., 2005, Bubble Column Reactors, Process Biochemestry. 40, 2263-2283.
Prasad A., 2000, Particle Imagem Velocimetry, Current Science, 79, 51-60.
Ruzicka M., Zahradnik J., Drahos J., Thomas N. H., 2001, Homogeneus –Heterogeneous Regime Transition in Buble Columns, Chem. Eng. Sci., 56, 4609-4621.
Sanchez-Forero D. I., Silva Jr J. L., Silva M. K., Bastos J. C. S. C., Mori M., 2013, Experimental and numerical investigation of gas-liquid flow in a rectangular bubble column with centralized aeration flow pattern, Chemical Engineering Transactions, 32, 1561-1566, DOI: 10.3303/CET 1332261.
Yang G.Q., Du Bing., Fan L.S., 2007, Bubble formation and dynamics in gas-liquid-solid fluidization, Chem. Eng. Sci., 60, 2-7.